

The theoretical angular-dependence plot from Eqs. (9)–(12) using the hyperfine constants given in Table II is shown in Fig. 5. The fit of the calculated lines with the partial angular-dependence experimental data is good.

Only the relative signs for each of the components in Table II can be determined from the analy-

sis. Since the magnetic moments of Cd^{111} and Cd^{113} are both negative, the contact interaction should have a negative sign if one assumes that there is no exchange polarization of the closed-shell orbitals of the cadmium ion. The negative signs in Table II and the M_s values shown in Fig. 4 are based on this assumption.

[†]Work supported by the U. S. Army Research Office, Durham, N.C., the Advanced Research Projects Agency, and the National Science Foundation.

*Present address: U. S. Army Construction Engineering Research Laboratory, Champaign, Ill.

[‡]Present address: Naval Research Laboratory, Washington, D.C.

¹M. M. Zaripov, V. S. Kropotov, L. D. Livanova, and V. G. Stepanov, *Fiz. Tverd. Tela* **10**, 325 (1968) [*Sov. Phys.-Solid State* **10**, 262 (1968)]; M. M. Zaripov, V. S. Kropotov, L. D. Livanova, and V. G. Stepanov, *Fiz. Tverd. Tela* **10**, 3438 (1968) [*Sov. Phys.-Solid State* **10**, 2722 (1969)].

²Yu. F. Mitrofanov, Yu. E. Pol'skii, and M. L. Falin, *Fiz. Tverd. Tela* **11**, 3555 (1969) [*Sov. Phys.-Solid State* **11**, 2976 (1970)].

³R. H. Borcherts and L. I. Lohr, Jr., *J. Chem. Phys.* **50**, 5262 (1969).

⁴P. Eisenberger and P. S. Pershan, *Phys. Rev.* **167**, 292 (1968).

⁵J. D. Kingsley and J. S. Prener, *Phys. Rev. Lett.* **8**, 315 (1962).

⁶R. H. Borcherts, T. Cole, and T. Horn, *J. Chem. Phys.* **49**, 4880 (1969).

⁷R. Valentin, *Phys. Lett. A* **30**, 344 (1969).

⁸T. P. P. Hall, W. Hayes and F. I. B. Williams, *Proc. Phys. Soc. Lond.* **78**, 883 (1961).

⁹U. Ranon and D. N. Stamires, *Chem. Phys. Lett.* **2**, 286 (1968).

¹⁰R. J. Richardson, Sook Lee, and T. J. Menne, *Bull. Am. Phys. Soc.* **17**, 147 (1972).

¹¹R. Gazzinelli and R. L. Mieher, *Phys. Rev.* **175**, 395 (1968).

¹²Y. H. Chu and R. L. Mieher, *Phys. Rev.* **188**, 1311 (1969).

¹³J. M. Baker and J. P. Hurrell, *Proc. Phys. Soc. Lond.* **82**, 742 (1963).

¹⁴C. P. Slichter, *Principles of Magnetic Resonance* (Harper and Row, New York, 1963).

¹⁵Program used is NONLINR which is available from the Statistical Library of the Purdue Computer Center.

The Effect of Pressure on Fe^{57} Hyperfine Fields in Ferromagnetic PdCo Alloys*

J. A. Cohen[†] and H. G. Drickamer

*Department of Physics, School of Chemical Sciences, and Materials Research Laboratory,
University of Illinois, Urbana, Illinois 61801*

(Received 2 August 1972)

The Fe^{57} hyperfine fields in a series of ferromagnetic PdCo alloys having cobalt concentrations between 5 and 15 at.% are measured by Mössbauer spectroscopy at 297°K and pressures up to 180 kbar. The pressure-dependent finite-temperature impurity hyperfine-field problem is parametrized in terms of the pressure dependence of the host Curie temperature, the zero-temperature hyperfine field, and the host-impurity coupling constant. In conjunction with previous data of Holzapfel *et al.* on the pressure dependence of the Curie temperatures, the present data are fitted within the molecular-field approximation with a positively pressure-dependent zero-temperature hyperfine field and a negatively pressure-dependent host-impurity coupling constant, the pressure derivatives being roughly composition independent. Implications of these results are discussed, and a comparison is made with the high-pressure Mössbauer data of Möller and Drickamer on PdFe alloys in the same composition range. Isomer-shift data are also presented briefly.

I. INTRODUCTION

The dilute alloy systems PdCo and PdFe have been the subject of much interest in recent years, stemming from the pioneering work of Constant,¹ Gerstenberg,² and Bozorth *et al.*³ on PdCo and Crangle⁴ on PdFe . The interest arises from (i) the "giant" magnetic moment associated with each impurity ($\sim 10 \mu_B$ in very dilute cases) and (ii) the extremely long range ($\sim 10 \text{ \AA}$) of the interaction which couples the impurity moments ferromagnetically. It is now understood that each Co or Fe impurity

maintains an on-site magnetic moment when dissolved in the Pd host,^{5,6} and because of the highly exchange-enhanced Pd susceptibility each impurity moment is able to polarize the surrounding Pd matrix out to large distances.^{6–11} The impurity-polarized-host complex then comprises the giant moment, and the polarized host carries the ferromagnetic interaction which couples the impurities indirectly.^{12–14} The dilute systems PdCo and PdFe are very similar. PdNi differs in that a Ni impurity cannot sustain a magnetic moment in the Pd host until a critical concentration of ~ 2 -at.% Ni

is reached; then the Ni moments appear and the alloy goes ferromagnetic concurrently.¹⁵

The Mössbauer effect has been used extensively to study these Pd-based alloy systems in both the dilute and nondilute regimes.¹⁶⁻³² Information has thereby been acquired on the strength and range of the ferromagnetic interactions, the statistical distribution and clustering of impurities, the concentration dependence and statistical smearing of the Curie temperatures, the temperature and field dependences of the bulk-alloy magnetizations, and the nature of the localized-impurity magnetic states and hyperfine interactions. The volume dependence of the magnetic properties of these systems has been investigated in magnetostriction,³³⁻³⁷ compressibility,^{38,39} and pressure-dependent resistance,³³ magnetoresistance,⁴⁰ and susceptibility^{33,41,42} experiments. The pressure dependence of the Fe⁵⁷ Mössbauer effect has been measured in this laboratory.⁴³⁻⁴⁵

The present work is concerned with the effects of pressure on the Fe⁵⁷ hyperfine fields, in zero external field at 297 °K, in a series of Pd_{1-x}Co_x alloys ranging from $x = 0.05$ to $x = 0.15$, at pressures up to 180 kbar. The effects are observed to be large, systematic, and nonlinear. The finite-temperature Fe⁵⁷-impurity hyperfine-field problem is parametrized in terms of five pressure-dependent quantities: the ferromagnetic Curie temperature T_C , the host magnetization σ_0 and local impurity moment μ_0 at $T=0$, the host-impurity coupling parameter ζ , and the impurity hyperfine coupling constant A . The impurity hyperfine field is seen to sense mainly T_C , $H_0 = A\mu_0$, and ζ , where H_0 is the hyperfine field at $T=0$. In conjunction with independent measurements of the pressure dependence of T_C for these alloys,⁴⁴ it is shown that the present data can be fitted semiquantitatively within the molecular-field approximation with a linearly positively pressure-dependent $|H_0|$ and a linearly negatively pressure-dependent $|\zeta|$, of the same magnitude for all alloys. Under the reasonable assumption that $d \ln H_0 / dp$ and $d \ln \zeta / dp$ must be roughly composition independent, the above fit is seen to be unique and demonstrates, we believe, the first observation of a pressure-dependent host-impurity coupling constant in a ferromagnetic metal.

A discussion is given of some implications of the above results. It is apparent that the Fe⁵⁷ impurity plays an active role in the effects observed here and does not probe the pressure-dependent magnetization of the host in a simple unobtrusive way. A comparison is made with pressure data for the alloy system PdFe in the same composition range as above.⁴⁵ The pronounced differences observed in the pressure-dependent properties of PdCo and PdFe are attributed to direct impurity-impurity

interactions, indicating that the present concentration regime cannot be considered dilute, as was previously done.⁴⁴ Isomer-shift data for the PdCo alloys are also presented briefly.

II. EXPERIMENTAL DETAILS

A. Sample Preparations

The Pd_{1-x}Co_x alloys (nominally 5-, 8-, 12-, and 15-at.% Co) were supplied by the Metal Science Group, Battelle Memorial Institute, Columbus, Ohio. The alloys were fabricated at Battelle by arc melting. Each charge was melted at least six times at 200 A and 30 V, held molten 20-25 sec, and quenched via water-cooled copper hearth. The weight loss in the melting process was less than 1% in each case. The arc-melted buttons were next cold rolled to about 0.1-in. thickness, homogenized in a vacuum furnace at 1125 °C for 24 h under an atmosphere of purified argon, and furnace cooled. There was no measurable weight loss. The samples were cold rolled again to 0.01 in. and were received thus at this laboratory. A Pd_{0.91}Co_{0.09} alloy was fabricated here in an induction furnace from the Pd_{0.92}Co_{0.08} and Pd_{0.88}Co_{0.12} alloys described above. The sample was contained in a recrystallized aluminum-oxide crucible, melted in an argon atmosphere with 13-14 kW of power for 10 min, then 8-9 kW for 1 min, and allowed to cool in the furnace. No weight loss was detected after the melting process.

Since the original alloys displayed somewhat messy Mössbauer spectra with broad lines (which could result from compositional inhomogeneities and a consequent variety of Mössbauer sites), these samples were submitted to additional homogenizing treatment along with that of the newly fabricated Pd_{0.91}Co_{0.09} alloy. (This homogenizing did, in fact, improve the spectra markedly.) Each sample was placed between two recrystallized aluminum-oxide chips and the resulting sandwich wrapped in molybdenum foil so that the sample itself would not contact the molybdenum. Then each bundle was sealed, with an argon atmosphere, in a separate quartz tube. These tubes were heated to 1200 °C in a resistance furnace and maintained there for 212 h, after which they were air then water cooled. The quartz tubes showed no evidence of darkening from sample vaporization. The new Pd_{0.91}Co_{0.09} alloy, now in the form of a button, was cold rolled to 0.01-in. thickness, then annealed in a boat similar to those described above, under argon, at 1000 °C for 5 min and 950 °C for 8 min. It cooled over a period of about 15 min. Flame-emission analysis for Co content at this point confirmed that, to within the accuracy of the measurement ($\Delta c/c \approx \pm 0.02$), all sample compositions were still nominal.

The alloys now had to be prepared as Mössbauer sources, of dimensions compatible with the high-pressure techniques to be used. First they were pressed and cold rolled to 0.001-in. thickness. Such thin samples are advantageous both for minimizing self-absorption of Mössbauer γ rays and for obtaining uniform reproducible pressures. A rectangular section 0.120 \times 0.014 in. was then fashioned, with a tab being left on one end. This rectangular section was suspended by its tab in a 1:1 $\text{NH}_4\text{OH-H}_2\text{O}$ electroplating solution which contained radioactive Co^{57} as a complex. (The Co^{57} was obtained from the Oak Ridge National Laboratory, Oak Ridge, Tenn. and from the New England Nuclear Corp., Boston, Mass.) A cathodic lead was attached to the tab, and with a platinum anode an applied voltage of 2 V produced a plating current of about 15 μA . The electroplating was continued until 1.5 mCi of Co^{57} had been deposited on the sample surface, usually a period of several days. The tab was then cut off.

The heat treatment necessary for diffusing the Co^{57} into the body of the sample, and for the final anneal, was found to require great care, as it was important to avoid contaminating the sample. Due to the small sample size (0.120 \times 0.014 \times 0.001 in.) a small amount of contamination from the sample holder could, and at first did, produce in the Mössbauer spectra very noticeable irreproducible effects, which were quite dependent on the amount of diffusion time. The following technique finally yielded reproducible consistent results: Several containers were fashioned from two 0.75-in. segments of 0.375- and 0.312-in.-diam molybdenum rod. Each segment was drilled out through most of its length, such that the i.d. of the large-diameter segment was a bit greater than the o.d. of the small-diameter one. Thus the larger piece formed a loosely fitting highly overlapping cover for the smaller piece. The containers were then chemically polished and heated in vacuum to 1000 $^\circ\text{C}$ for 1 h for degassing. Next some aluminum oxide wool was cleaned in hot aqua regia, filtered, stuffed into the Mo containers, and heated in vacuum at 1000 $^\circ\text{C}$ for $\frac{1}{2}$ h. The wool which emerged was clean, fluffy, and pure white. The radioactive samples were then set on wool in the centers of separate Mo containers, held in place by more wool, and enclosed with the Mo covers. The containers were put in a quartz tube which was sealed into a diffusion-pump vacuum system and surrounded by a cylindrical resistance furnace. The samples were thus "open" to the vacuum, yet shielded from the quartz by the closed Mo containers and prevented from contacting the Mo by the aluminum oxide wool. The heat treatment was carried out under a vacuum of 2×10^{-7} Torr. The heating was performed slowly so that the vacuum

was always better than 2×10^{-6} Torr. The diffusion was accomplished at 800 $^\circ\text{C}$ for 12 h, the temperature was brought up to 950 $^\circ\text{C}$ for 1 h for annealing, and a slow cooling process was then begun. The cooling period was divided approximately into three equal time intervals, the first ending just above the Curie temperature, the second just below the Curie temperature, and the third at room temperature. Since the highest Curie temperature encountered was ~ 150 $^\circ\text{C}$, most of the time was spent at low temperatures. The intent was to attempt to form large domains, and thus reduce to a minimum possible complications resulting from domain-wall effects. With the above careful technique, cooling periods of 10 and 25 days yielded identical Mössbauer results. The radioactive foil was now cut into three pieces, to be used in three separate pressure runs. Each piece was 0.040 \times 0.014 \times 0.001 in. and contained ~ 0.5 mCi of radioactivity.

The possibility of having altered the alloy compositions through introduction of the radioactive Co must be considered, especially since some non-radioactive Co^{59} was included along with the Co^{57} . A 1.5-mCi sample of Co^{57} radioactivity ($t_{1/2} = 270$ days) requires that 2×10^{15} Co^{57} nuclei be present. According to the manufacturer, there may have been several times this amount of Co^{59} also present, as well as some Fe^{57} depending on the age of the material. From the known lattice constant of the alloy (or from the density) it can be shown that a sample of the size used here contains $\sim 2 \times 10^{18}$ atoms. Thus about 0.2- to 0.3-at.% Co was added to each sample. Hence we take the Co content of the Mössbauer sources to be (5.2, 8.2, 9.2, 12.2, and 15.2) ± 0.3 -at.% Co. The Fe^{57} contained in the initial radioactive solution was not plated onto the sample, since Fe does not complex with the electroplating solution. Thus the Fe^{57} content of each sample depends on the amount of time elapsed since the plating. After one year, a sample would be ~ 0.06 -at.% Fe^{57} .

The PdCo alloys thus prepared are random substitutional alloys⁴⁶ in polycrystalline form. Our observations therefore sense an average over all directions of hyperfine field. Due both to the rolling process in the formation of the foil and to the demagnetizing energy of the foil, however, it is unlikely that the orientations of the crystallites are truly random.⁴⁷ Such directional phenomena do not affect the quantities of interest here, which are the *magnitudes* of the fields $|H_i|$.

The single-line absorber used in this work was a 0.00025-in. thick No. 303 stainless-steel foil enriched with 1.5 mg/cm² of Fe^{57} . The enriching was done by electroplating a layer of Ni, then Fe^{57} , onto the foil surface and heating for 24 h under vacuum at 700 $^\circ\text{C}$. The process was then repeated

until the desired Fe^{57} area density had been achieved. The Ni helped the Fe^{57} adhere to the foil surface, and was also necessary to keep the alloy in a nonmagnetic phase. The Fe^{57} was obtained from Oak Ridge.

B. High-Pressure Techniques

The high-pressure techniques employed here have been described in detail elsewhere.^{43,48,49} An essential modification was made, however, in the accommodation of the foil samples. The high-pressure cell is pictured in Fig. 1. It was found that pressure runs were markedly improved (with regard to the magnitude of the pressures obtained and their reproducibility) when the button backing the foil was made of the same 85-wt% boron-15-wt% lithium-hydride mix as the outer pellet, instead of pyrophyllite as was used previously.⁴⁹ The cell shown in Fig. 1 is placed between the flats of Bridgman anvils and compressed uniaxially in a hydraulic press. (See Fig. 2 of Ref. 48.) Friction prevents the B-LiH from squirting out between the anvil flats and the B-LiH transmits the applied force quasi-hydrostatically to the sample.⁵⁰

It should be appreciated that the foil sample sits *on edge* relative to the direction of applied force by the press. The γ rays emitted from the foil source have only to pass through a small thickness of low-absorbing B-LiH in order to reach the Mössbauer spectrometer. The limiting pressures for this work (~ 200 kbar) are set not by the maximum attainable sample pressures, but by plastic flow of the anvil faces which eventually bows them and cuts off the Mössbauer radiation.

The pressure calibration of the present high-pressure cell was originally determined with x rays, using the high-pressure x-ray techniques of Perez-Albuerne *et al.*⁵⁰ Periodic checks of the quality of the critical cell-loading technique were performed by loading a bismuth foil, measuring

resistance vs applied pressure, and noting discontinuities at the 25- and 75-kbar transition points.

C. Mössbauer Techniques

The Mössbauer spectrometer employed in this work has been described in Ref. 48, and in more detail in Ref. 43. The moving-absorber configuration was used here, the source being the pressurized sample under study. The computer program for fitting the raw Mössbauer data was essentially that of Chrisman and Tumolillo.⁵¹ The fitted quantities of most interest here are the line positions, since the magnitude of the six-line splitting is proportional to the Fe^{57} hyperfine field $|H_i|$, and the centroid of the six-line spectrum gives the isomer shift. (There were no electric-quadrupole effects observed in this work.) The spectra of each pressure run were calibrated against a standard to determine the hyperfine-field scale (the number of kOe corresponding to an observed line splitting) and the isomer-shift energy scale (the number of mm/sec of Doppler shift corresponding to the width of each channel of the multichannel analyzer memory). The standard was a source of Fe^{57} in ferromagnetic iron metal, at atmospheric pressure. For each pressure run this iron spectrum was taken with the same absorber and the same absorber motion as used in the run itself. The ratio of the line splittings for the spectrum of a given sample to the splittings for iron (in channel numbers) is then the ratio of $|H_i|_{\text{sample}}$ to $|H_i|_{\text{iron}}$, and the latter was taken to be 330 kOe.^{52,53} The data of Preston *et al.*⁵² on the relative positions of the iron lines in mm/sec (at 294 °K) were used to determine the isomer-shift energy calibration, i. e., the number of mm/sec per channel.

III. DATA AND INTERPRETATION

A. Data

Some typical Mössbauer spectra are shown in Figs. 2(a), 2(b), and 2(c). All data were taken at constant temperature $T=297$ °K. The solid curves are computer fits (superpositions of Lorentzians) to the experimental data points. The effect of pressure on the hyperfine field for $\text{Pd}_{0.91}\text{Co}_{0.09}$ is seen to be quite dramatic. We wish to stress the fact that *all pressure effects observed here are reversible*, i. e., upon release of pressure the hyperfine fields return very close to their initial $p=0$ values, the $x=0.08$ and $x=0.09$ spectra collapsing back to single lines. Figure 3 shows the pressure and volume dependences of the Fe^{57} hyperfine fields, at 297 °K, observed for the four alloys in this experiment. [No hyperfine field was observed for $\text{Pd}_{0.95}\text{Co}_{0.05}$, since it remained paramagnetic at all pressures (cf. Table I).] The solid lines in Fig. 3 are simply smoothed curves drawn

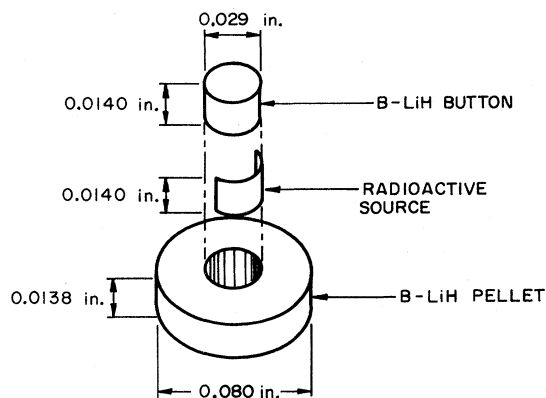


FIG. 1. High-pressure cell.

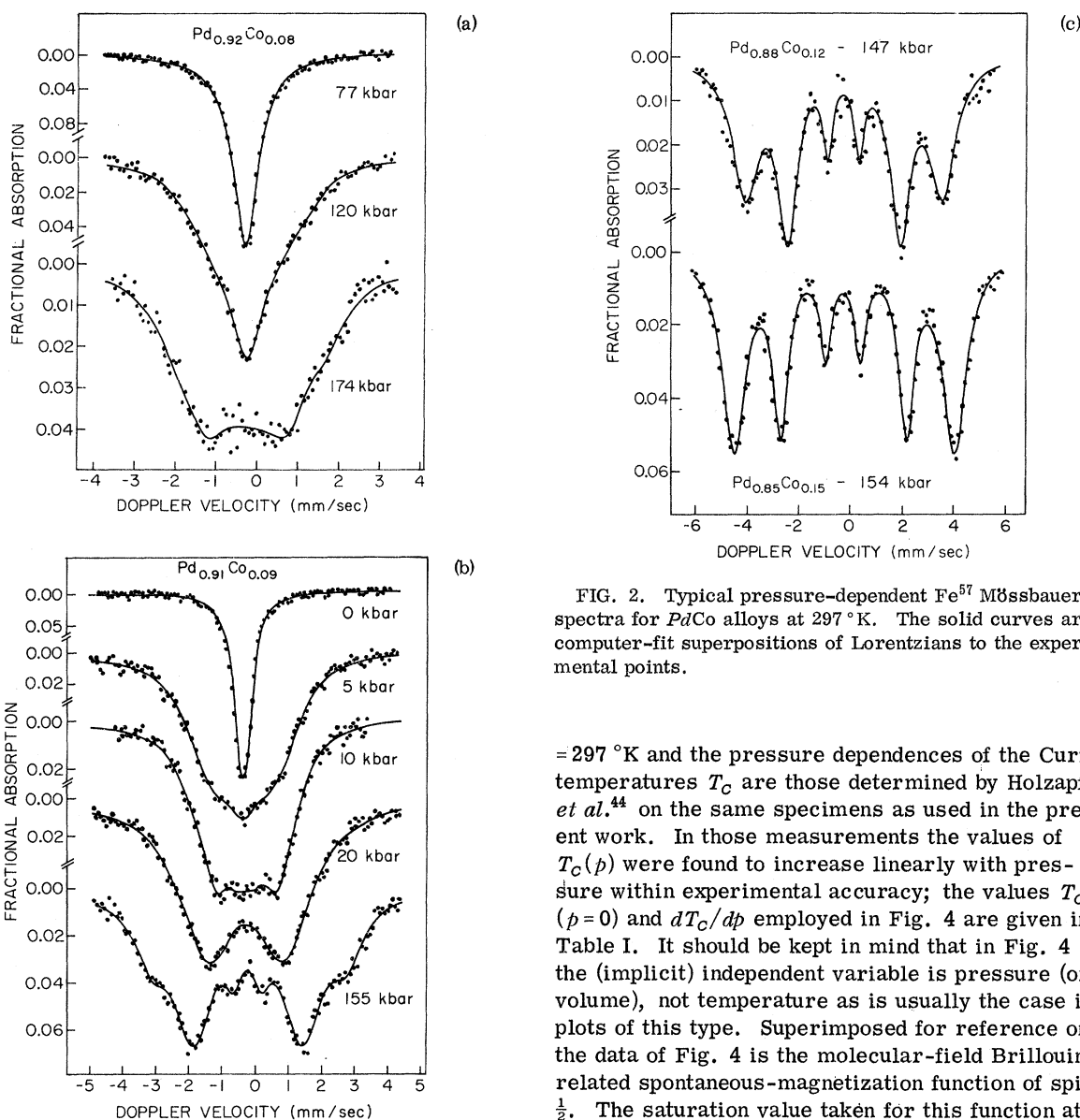


FIG. 2. Typical pressure-dependent Fe^{57} Mössbauer spectra for PdCo alloys at 297 °K. The solid curves are computer-fit superpositions of Lorentzians to the experimental points.

through the data points for convenience of later analysis (cf. Fig. 4) and do not represent a theoretical fit to the data. The volume vs pressure relation used in the abscissa of Fig. 3 is not critical to the present analysis and is shown mainly for interest. The relations V/V_0 vs p for these alloys were obtained from the shock-wave data of Rice *et al.*⁵⁴ on pure Pd and Co.⁴³ Since V/V_0 is only $\sim 0.5\%$ less for Pd than for Co at $p = 200$ kbar, the curves V/V_0 vs p for the alloys, which are assumed to lie proportionally between those of pure Pd and pure Co, are virtually the same to the degree of accuracy required here.⁵⁵

The data of Fig. 3 are replotted in Fig. 4 as $H_i(p)$ vs $T/T_C(p)$ for each alloy, where $T = \text{const}$

$= 297$ °K and the pressure dependences of the Curie temperatures T_C are those determined by Holzapfel *et al.*⁴⁴ on the same specimens as used in the present work. In those measurements the values of $T_C(p)$ were found to increase linearly with pressure within experimental accuracy; the values $T_C(p=0)$ and dT_C/dp employed in Fig. 4 are given in Table I. It should be kept in mind that in Fig. 4 the (implicit) independent variable is pressure (or volume), not temperature as is usually the case in plots of this type. Superimposed for reference on the data of Fig. 4 is the molecular-field Brillouin-related spontaneous-magnetization function of spin $\frac{1}{2}$. The saturation value taken for this function at $T/T_C = 0$ is that determined by Nagle *et al.*,¹⁶ who have shown that the Fe^{57} hyperfine field in $\text{Pd}_{1-x}\text{Co}_x$ for $T/T_C \ll 1$, at 1 atm, is nearly independent of composition in the range $0.03 \leq x \leq 1.00$, with the value $H_i(T/T_C \approx 0) = -308 \pm 5$ kOe.

B. Parametrization

In order to discuss the significance of Fig. 4, we first review briefly the phenomenological parameters involved. The thermal behavior of the spontaneous magnetization σ of a ferromagnet in zero external field is described by a relation of the form

$$\sigma(T) = \sigma_0 f(T/T_C), \quad (1)$$

where $\sigma_0 \equiv \sigma(T=0)$, f is the "spontaneous-magnetization function" which falls from $f(0) = 1$ to $f(1)$

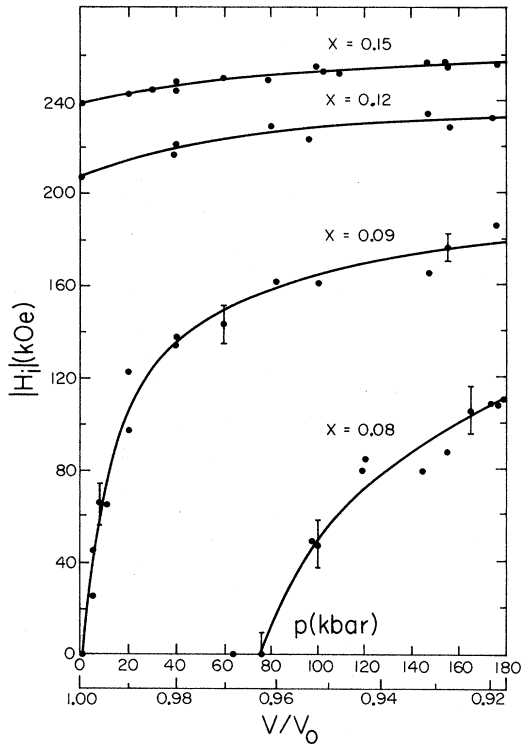


FIG. 3. Pressure and volume dependences of the Fe⁵⁷ hyperfine fields in Pd_{1-x}Co_x alloys at 297 °K. Dots mark the hyperfine field values obtained from the line splittings of computer-fit Mössbauer spectra. Typical error bars are shown for $x = 0.08$ and 0.09 ; experimental uncertainties for $x = 0.12$ and 0.15 are the size of the dots themselves. The pressures are accurate to $\pm 5\%$ – 10% . The solid lines are simply smoothed curves drawn through the data points.

$= 0$, and T_C is the ferromagnetic Curie temperature.^{58,57} In the molecular-field approximation the function f is related to the Brillouin function B_S having the appropriate “effective spin” S . Thus, under pressure at constant temperature, the major effects on $\sigma(T)$ occur via $\sigma_0(p)$ and $T_C(p)$. Smaller effects are possible from a pressure dependence of the function f itself, for example through a pressure dependence of S in the molecular-field approximation, but both σ_0 and T_C are much more strongly dependent on S than is the function f .⁵⁷ For our purposes any pressure dependence of the function f can be neglected.

The hyperfine field H_i observed at the nucleus of a *homogeneous* parent atom within a ferromagnet (e.g., at an Fe⁵⁷ site in iron metal or Ni⁶¹ in nickel) also obeys a relation of the form

$$H_i(T) = H_0 f(T/T_C), \quad (2)$$

where $H_0 \equiv H_i(T=0)$ and the function f is nearly identical with that of Eq. (1). Disregarding relaxation effects,²⁰ the T_C of Eq. (2) is the same as that

of Eq. (1). Thus $H_i(T)/H_0 \approx \sigma(T)/\sigma_0$, and the hyperfine field “follows” the spontaneous magnetization of the sample as a function of temperature. Since for the homogeneous case the “spin” associated with the parent atom is simply the magnetization per atom of the host, the nearly constant ratio $H_i(T)/\sigma(T) \approx H_0/\sigma_0 \approx A$ is just the hyperfine coupling constant, i.e., the magnitude of “field” seen by the nucleus per unit of “spin” associated with its parent atom. From Eq. (2) the pressure dependence of $H_i(T)$ at constant T is determined by $H_0(p)$ and $T_C(p)$, but $H_0(p)$ is the product of $\sigma_0(p)$ and $A(p)$. Hence in observing hyperfine fields the complication arises that the coupling between the spin of the parent atom and the field sensed by the nucleus can be, and generally is, pressure dependent.^{58,59}

The situation in which the hyperfine field is measured at the nucleus of an *impurity* atom in a ferromagnetic host (for example, Fe⁵⁷ in nickel) is substantially more complex. We consider here only the case in which the impurity atom has a well-defined localized moment, as is often the case for the Fe⁵⁷ impurity. The thermally averaged moment μ associated with the impurity atom has a temperature dependence given by

$$\mu(T) = \mu_0 g(T/T_C), \quad (3)$$

where, analogously to Eq. (1), $\mu_0 \equiv \mu(T=0)$ and the function $g(T/T_C)$ also decreases from 1 at $T=0$ to 0 at $T=T_C$. In general, however, $g(T/T_C) \neq f(T/T_C)$; the impurity magnetization does not follow the host magnetization with temperature and can deviate significantly from it. The reasons, within the molecular-field picture, are twofold: (i) the impurity atom may have a different spin than that of the average host atom, hence will respond differently to the molecular or exchange field driving it; and (ii) the exchange field driving the impurity can be different from the average molecular field driving the host. Both effects are included in a phenomenological quantity ζ which parametrizes the strength of the impurity’s thermal response to the host magnetization f .^{60–64} Thus the function g depends on the function f via a relation involving the parameter ζ : $g(T/T_C) = g[\zeta, f(T/T_C)]$. This

TABLE I. Values of $T_C(p=0)$ and dT_C/dp for the present Pd_{1-x}Co_x alloys, determined by Holzapfel *et al.*^a

x (± 0.005)	$T_C(p=0)$ (°K)	dT_C/dp (°K/kbar)
0.05	196 \pm 2	+0.10 \pm 0.02
0.08	283 \pm 2	+0.20 \pm 0.03
0.09	292 \pm 2	+0.23 \pm 0.03
0.12	356 \pm 2	+0.37 \pm 0.04
0.15	417 \pm 2	+0.45 \pm 0.06

^aReference 44.

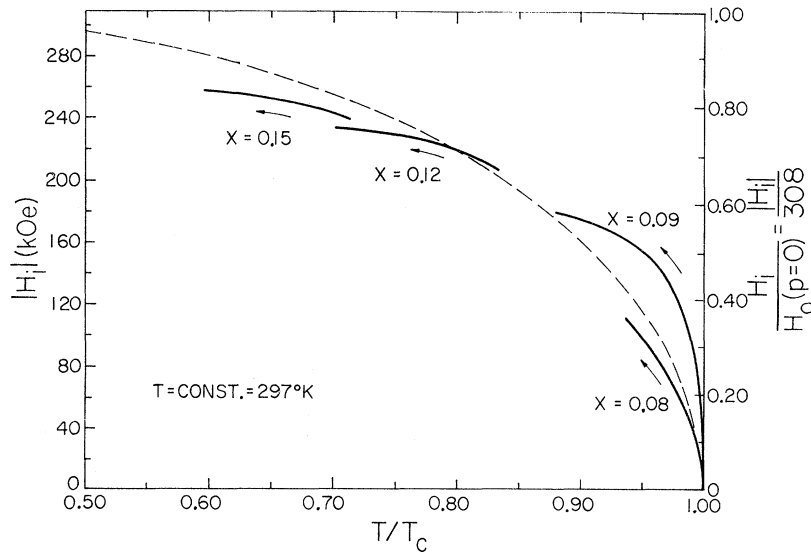


FIG. 4. Experimental hyperfine fields vs T/T_C for $\text{Pd}_{1-x}\text{Co}_x$ alloys at 297°K, with pressure the implicit variable. $H_i(p)$ data are the smoothed experimental curves of Fig. 3 and $T_C(p)$ data are taken from Table I. The right-hand ordinate is normalized to $|H_0(p=0)| = 308$ kOe as described in the text. The dashed curve is the molecular-field spontaneous-magnetization function of spin- $\frac{1}{2}$. The arrows indicate the direction of increasing pressure.

relation is easily calculated in the molecular-field approximation and works well if conduction-electron contributions to the impurity moment are small. For a strong response (Fe^{57} in Ni) g lies above f , saturating more quickly as T drops below T_C , while for a weak response (Mn^{55} in Fe) g lies below f and may be sigmoid shaped.^{63,60} Under pressure, then, one must now consider $\zeta(p)$, the pressure dependence of the relative host-impurity magnetic coupling. As before, the hyperfine field follows the magnetization associated with the parent atom as a function of temperature, although the latter quantity is no longer tracking the magnetization of the host. Thus

$$H_i(T) = H_0 g(T/T_C), \quad (4)$$

whence, using Eq. (3), the hyperfine coupling constant is $A = H_i(T)/\mu(T) = H_0/\mu_0$. In this picture, then, the host magnetization $\sigma(T)$ is coupled to the local impurity magnetization $\mu(T)$ via ζ , and $\mu(T)$ is in turn coupled to the impurity hyperfine field $H_i(T)$ via A .

There are thus five phenomenological parameters whose pressure dependence is expected to be of primary importance in interpreting pressure effects on the hyperfine fields associated with well-defined localized-moment impurities in ferromagnetic hosts: T_C , σ_0 , μ_0 , ζ , A . The pressure-dependent quantities most directly related to the observed hyperfine fields are: T_C , $H_0 = A\mu_0$, and ζ . On the other hand, in homogeneous cases the relevant quantities are: T_C and $H_0 = A\sigma_0$, and the parameter ζ does not appear. Information on interactions within the host are given by the pressure (or volume) dependences of T_C and σ_0 ; the pressure dependence of μ_0 , A , and ζ are properties

of the impurity atom itself and of its interaction with the host.

C. Results

We now show, with reference to the parameters outlined above, that it is possible to explain the essential features of the data of Fig. 4 by use of a simple molecular-field picture. Semiquantitative estimates of the pressure dependences of the relevant parameters are obtained. Quantitative determinations, however, will be seen to require further temperature-dependent data which are not currently available. In Fig. 5 we plot a family of impurity response functions $g(T/T_C)$ for impurity spin- $\frac{1}{2}$, parametrized by the relative host-impurity coupling constant ζ , referenced to the host spontaneous-magnetization function $f(T/T_C)$ of spin- $\frac{1}{2}$, all within the molecular-field approximation. $g(T/T_C)$ coincides with $f(T/T_C)$ here when $\zeta = 1.0$. The function $g(T/T_C)$ is related to $f(T/T_C)$ in the molecular-field approximation according to

$$g(T/T_C) = B_S \left(\zeta \frac{f(T/T_C)}{T/T_C} \right), \quad (5)$$

where S' is the impurity spin and B_S is a Brillouin function.^{60,63} The host spontaneous-magnetization function $f(T/T_C)$ need not be expressed within the molecular-field approximation here, but can be the exact experimental function $\sigma(T)/\sigma_0$. Callen *et al.*⁶¹ note that the molecular-field theory is much more accurate for the impurity than for the host,⁶⁵ so Eq. (5) should work well for $g(T/T_C)$ even when the molecular-field theory does not give a good representation of $f(T/T_C)$. [Equation (5) is *exact*, however, only in the weak coupling limit.⁶²] For simple illustrative purposes in Fig. 5 we use the molecular-field theory for f as well as for g (see Appen-

dix).

By considering the functions $g(T/T_C)$ of Fig. 5 to represent possible values of $H_i(T)/H_0$ according to Eqs. (4) and (5), a series of hypothetical pressure-dependent curves can be generated by use of (i) the values $T/T_C(p)$ for each alloy from the data of Table I with $T = \text{const} = 297^\circ\text{K}$ (as was done in Fig. 4) and (ii) an assumed $\zeta(p)$. For example, $\zeta(p) = \text{constant}$ implies that all curves $H_i(T, p)/H_0(p)$ coincide with the same function $g(T/T_C)$ as $T/T_C(p)$ decreases with pressure for each alloy. The dashed segments in Fig. 5 illustrate the effect of a linear decrease of ζ with pressure, from $\zeta = 1.0$ at 0 kbar to $\zeta = 0.6$ at 180 kbar. For purposes of comparison with the data of Fig. 4, however, it is necessary to convert the dashed curves of Fig. 5 to the form $H_i(T, p)$ vs $T/T_C(p)$, i. e., to multiply each dashed segment by $H_0(p)$. The pressure dependence of H_0 is most readily determined for the alloy with lowest T/T_C , since $H_i(T)$ there has greatest sensitivity to changes of H_0 . $H_0(p)$ has thus been "fitted" for Pd_{0.85}Co_{0.15} by requiring that the model curve reproduce the experimental ratio $[H_i(p = 180)/H_i(p = 0)] = 1.08$ for this alloy (pressure units in kbar), with a linear pressure dependence. The solid segments in Fig. 5 show the effect of applying this same $H_0(p)$ to all four alloys. The right-hand ordinate of Fig. 5 should be compared to the right-hand ordinate of Fig. 4. The similarities to the experimental curves of Fig. 4 are apparent: The $x = 0.09$ alloy shows a very dramatic pressure effect; the various $H_i(T, p)$ segments are not continuous, with the $x = 0.08$ curve lying below the $x = 0.09$ curve and the high-pressure region of the $x = 0.12$ curve falling below the low-pressure overlapping T/T_C region of the $x = 0.15$ curve; the

over-all increase of $|H_i|$ is greater for the $x = 0.12$ alloy than for $x = 0.15$ and greater for $x = 0.09$ than for $x = 0.08$; all curves have qualitatively the correct shapes, increasing most rapidly at the lower pressures and tending to level off at the higher pressures. The values of the two pressure-dependent parameters employed in Fig. 5 are $d \ln \zeta / dp = -2.8 \times 10^{-3} / \text{kbar}$ and $d \ln H_0 / dp = +1.1 \times 10^{-3} / \text{kbar}$, the same for all alloys. The most glaring fault of the model curves of Fig. 5 is the insufficient depression of the $x = 0.08$ curve below the $x = 0.09$ curve. This difficulty can be rectified somewhat by assuming a larger negative pressure dependence to ζ , and the effect of doing so is shown in Fig. 6, where $\zeta = 0.5$ at 180 kbar and $H_0(p)$ is determined by the same criterion as above. The situation is indeed improved for $x = 0.08$ and $x = 0.09$ but is worsened for $x = 0.12$ and $x = 0.15$, because the experimental curves do not show a decrease of $|H_i|$ at the highest pressures. In Fig. 6, $d \ln \zeta / dp = -3.7 \times 10^{-3} / \text{kbar}$ and $d \ln H_0 / dp = +1.7 \times 10^{-3} / \text{kbar}$.

The model curves of Figs. 5 and 6 are not detailed quantitative reproductions of the experimental data for several reasons, although in view of the simplicity of the molecular-field model used and the paucity of pressure-dependent parameters employed the qualitative picture is indeed satisfactory. For example, we have included no variation of the parameters $\zeta(p)$ and $H_0(p)$ with composition, and have moreover assumed linear pressure dependences for these quantities. The major obstacle to a more quantitative analysis of the present pressure-dependent data, however, lies in the lack of a satisfactory $p = 0$ "baseline" for each alloy from which a realistic set of the ζ -dependent functions $g(T/T_C)$ can be obtained from Eq. (5) or from

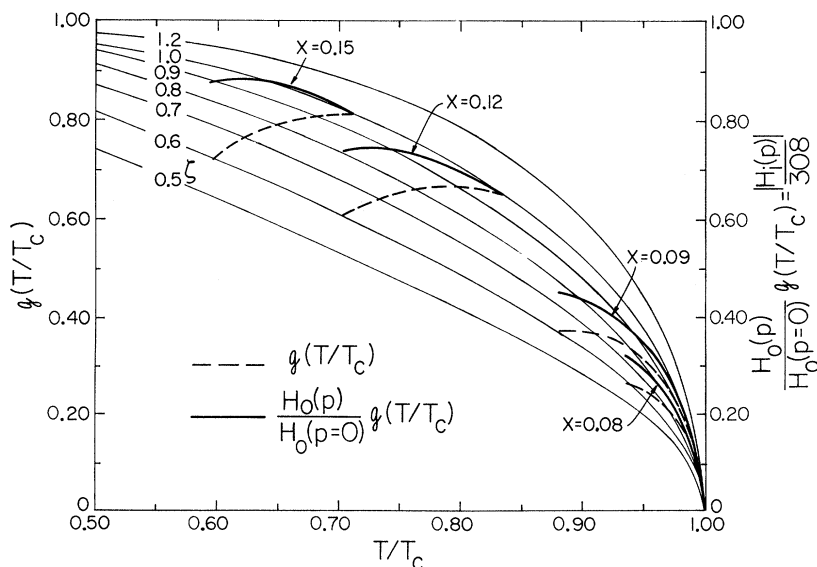


FIG. 5. Model curves of normalized hyperfine fields vs T/T_C . Light lines: molecular-field impurity response functions, parameterized by ζ as described in the text. Dashed lines: hypothetical pressure-dependent impurity response curves using $T_C(p)$ from Table I and $\zeta(p)$ as described in the text. Heavy lines: dashed lines modified by pressure-dependent $H_0(p)$ as described in the text, representing normalized hyperfine field curves to be compared to the right-hand ordinate of Fig. 4.

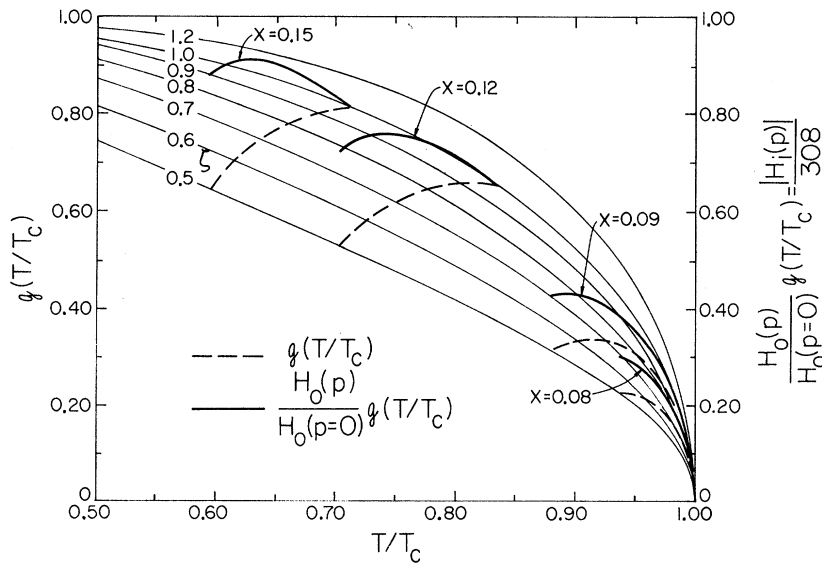


FIG. 6. Model curves of normalized hyperfine fields vs T/T_C , with different pressure dependence of the parameters ζ and H_0 from those of Fig. 5. See text.

Eq. (A3). Our use of the molecular-field spontaneous-magnetization function of spin- $\frac{1}{2}$ in conjunction with $\zeta(p=0)=1.0$ for all alloys is clearly inadequate, particularly for $x=0.09$ as seen in Fig. 4. It should be appreciated that the actual $p=0$ isobars of $H_i(T)/H_0$ for the various alloys probably do not lie on a single continuous curve, especially if $\zeta(p=0)$ is composition dependent. What is required here is the experimental temperature-dependent $H_i(T)$ for each alloy at $p=0$, covering at least the range of T/T_C as is spanned in each case by the pressure data of Fig. 4.

In Fig. 7 we attempt a more realistic treatment of the $x=0.08$ and $x=0.09$ data in the interesting region $T/T_C \lesssim 1$ by using the curve $H_i(T)/H_0$ vs T/T_C for Fe^{57} in nickel as a $p=0$ baseline. This curve nearly coincides with our $x=0.09$ data in the low-pressure region, and therefore is perhaps a reasonable approximation to the $p=0$ baseline for $x=0.09$. The background grid in Fig. 7 consists of the experimental curve of Dash *et al.*⁶³ for Fe^{57} in nickel [= $g_0(T/T_C)$] and a family of the ζ -dependent curves $g(T/T_C)$ calculated from Eq. (A3) with $S'=\frac{3}{2}$. This value for the Fe impurity spin is sug-

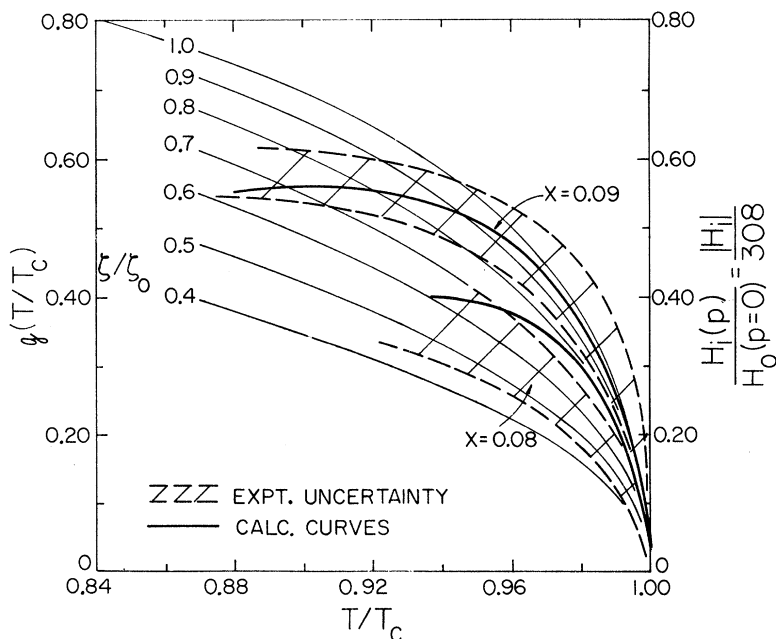


FIG. 7. Model and experimental curves of normalized hyperfine fields vs T/T_C for $\text{Pd}_{0.92}\text{Co}_{0.08}$ and $\text{Pd}_{0.91}\text{Co}_{0.09}$ at 297°K, using the experimental baseline for Fe^{57} in nickel from Ref. 63 as described in the text.

gested by the fact that the moment localized at an Fe site in both pure Pd and pure Co (and therefore probably in PdCo) is about $3 \mu_B$.^{5,6,72} (The use, for simplicity, of $S' = \frac{1}{2}$ in Figs. 5 and 6 does not affect the semiquantitative results obtained there.) The hatched areas indicate the ranges of uncertainty of our data for the $x=0.08$ and $x=0.09$ alloys. The solid lines show the fits obtained using $\zeta(p)$ from Fig. 6 and $H_0(p)$ from Fig. 5 for both alloys, indicating that these parameters are also semiquantitatively valid here.

The conclusions obtainable from the current analysis are now discussed. As mentioned above, the three parameters whose pressure dependences directly affect the pressure dependence of the impurity hyperfine field are T_C , H_0 , and ζ . T_C has been measured independently for each alloy here and its effects included in Fig. 4. Thus, in interpreting Fig. 4, one is left to consider $H_0(p)$ and $\zeta(p)$, separately for each alloy. With no constraints these parameters allow more than enough freedom to fit the data (given an appropriate $p=0$ baseline in each case), and in fact satisfactory fits can be obtained solely by consideration of $H_0(p)$ alone, or $\zeta(p)$ alone, independently for each alloy. A strong constraint is imposed, however, by the fact that $H_0(p)$ is not likely to be very composition dependent. The reason is that the Fe⁵⁷ $H_0(p=0)$ has been found to be virtually independent of composition (within several percent) over the entire composition range of Pd_{1-x}Co_x,^{16,17,25} while the average moment per atom of the alloy and the average moment per Co atom vary considerably with composition.³ Thus the magnitude of $H_0(p=0)$ must be determined primarily by local phenomena, which are insensitive to the $T=0$ bulk magnetization of the alloy and sense mainly the local Fe moment, which is stably saturated at $\sim 3 \mu_B$. The pressure derivative of a locally determined H_0 must also be locally determined, and hence cannot be composition dependent either. As for the parameter $\zeta(p)$, it is reasonable to expect some, but not a large, composition dependence in the limited range of interest here, $0.08 \leq x \leq 0.15$. We therefore assume that, to lowest order, both $d \ln H_0/dp$ and $d \ln \zeta/dp$ are roughly the same for all alloys.

Given the assumption of approximate composition independence for $H_0(p)$ and $\zeta(p)$, the data of Fig. 4 unambiguously imply (i) a positive pressure dependence for $|H_0|$ and (ii) a negative pressure dependence for $|\zeta|$. Any attempt to account for the suppression of the $x=0.08$ curve below the $x=0.09$ curve or the flattening of the $x=0.09$ curve in the high-pressure region by a negatively pressure-dependent $|H_0(p)|$ results in a decreasing $|H_i(p)|$ for $x=0.12$ and $x=0.15$, contrary to observation. In order to achieve consistency with the $x=0.12$ and $x=0.15$ data, the above characteristics

of the $x=0.08$ and $x=0.09$ curves must be determined primarily by a negatively pressure-dependent $|\zeta|$, thus requiring a positively pressure-dependent $|H_0|$, as seen in Figs. 5 and 6. The data indicate $d \ln H_0/dp \approx + (1.0 \pm 0.5) \times 10^{-3}/\text{kbar}$ and $d \ln \zeta/dp \approx - (3 \pm 1) \times 10^{-3}/\text{kbar}$, with $|d \ln \zeta/dp|$ being perhaps somewhat composition dependent, increasing as x decreases. We believe these results to constitute the first observation of the pressure dependence of an impurity-host coupling constant in a ferromagnetic metal.

IV. DISCUSSION

A. $H_0(p)$

The value found here for $d \ln H_0/dp$ agrees in both sign and magnitude with that found by Raimondi and Jura⁶⁶ for Fe⁵⁷ in cobalt at room temperature: $d \ln H_i/dp = +0.6 \times 10^{-3}/\text{kbar}$. Since T_C for cobalt is 1395 °K (fcc phase) or 1130 °K (hcp phase),⁶⁷ T/T_C for the above measurement ≈ 0.21 or 0.26, respectively. Contributions to $H_i(p)$ from $\zeta(p)$ at these values of T/T_C should be small, although not necessarily negligible, so the above pressure dependence of $H_i(p)$ represents mainly the effect of $H_0(p)$. [In cobalt $dT_C/dp = 0 \pm 0.05$ °K/kbar,⁶⁸ so $T_C(p)$ has no effect on $H_i(p)$ here, particularly for these low values of T/T_C .] As mentioned, the compressibilities of the PdCo alloys are very close to that of pure Co, so the present value $d \ln H_0/d \ln V = -1.9 \pm 1.0$ is in rough agreement with that for Fe⁵⁷ in Co, where $d \ln H_0/d \ln V \sim -1.1$.

If in fact the Fe moment is well localized here, it is expected that μ_0 should not be very pressure sensitive, and since $H_0(p) = A(p)\mu_0(p)$, the pressure dependence of H_0 is then determined mainly by the pressure dependence of the hyperfine coupling constant A . $d \ln A/dp$ has been shown to be positive for Fe⁵⁷ in iron,^{69,49,58} the main reason being^{59,70} that expansion of the d -like wave functions with pressure increases the core polarization, thus increasing the hyperfine field per spin. Our positive $d \ln H_0/dp$ could well reflect a similarly positive $d \ln A/dp$ for Fe⁵⁷ as an impurity in the PdCo alloys. The pressure insensitivity of the Fe moment μ_0 follows from the work of Moriya,⁷¹ which indicates that localized moments, when in the saturation regime, are very stable. Neutron diffraction measurements show the local Fe moment in Pd and Co to be of order $3 \mu_B$,^{5,6,72} which is about the maximum possible considering a local Fe configuration $\sim 3d^7 4s^1$ as is indicated by the Fe⁵⁷ isomer shifts in these metals.^{59,73-75} Thus, taking $g=2$, the Fe impurity moment is essentially saturated and therefore stable with respect to environmental perturbations. Undoubtedly, this is also the reason for the insensitivity of the Fe moment

(and hyperfine field) to compositional changes in the $T=0$ host magnetization of $\text{Pd}_{1-x}\text{Co}_x$, as noted earlier.

B. $\zeta(p)$

The phenomenological host-impurity coupling parameter ζ of Eq. (5) is defined as the ratio of the exchange energy of the impurity to the ferromagnetic ordering energy of the host,

$$\zeta = g'S'\mu_B H_0^{\text{ex}}/kT_C, \quad (6)$$

where H_0^{ex} is the exchange field at $T=0$ acting on the impurity moment $\mu_0 = g'S'\mu_B$.⁶⁰ Thus the pressure (or volume) dependence of the impurity exchange energy is

$$\frac{d \ln E^{\text{ex}}}{dp} = \frac{d \ln \zeta}{dp} + \frac{d \ln T_C}{dp} \quad (7)$$

or

$$\frac{d \ln H_0^{\text{ex}}}{dp} = \frac{d \ln \zeta}{dp} + \frac{d \ln T_C}{dp} - \frac{d \ln \mu_0}{dp}. \quad (8)$$

From above, $d \ln \zeta/dp \sim -3 \times 10^{-3}/\text{kbar}$ for these alloys, while from Table I $d \ln T_C/dp$ ranges from $\sim + (0.7 \text{ to } 1.1) \times 10^{-3}/\text{kbar}$. From Eq. (7) it is thus apparent that, in addition to the impurity's becoming *relatively* decoupled from the host as pressure increases (because $d \ln \zeta/dp < 0$), the exchange energy of the impurity is decreasing *absolutely* with pressure. If, from previous discussions, it is assumed that the impurity moment is relatively insensitive to compression, then $d \ln \mu_0/dp \sim 0$ in Eq. (8), and it is also seen that the exchange field driving the impurity is decreasing in an absolute sense with pressure.

C. $T_C(p)$

The pressure dependence of the Curie temperatures of these alloys has already been discussed by Holzapfel *et al.* in Ref. 44. However, further discussion is given below in conjunction with the PdFe alloys.

D. PdFe

The pressure dependences of the Curie temperatures and Fe^{57} hyperfine fields of the alloys $\text{Pd}_{1-x}\text{Fe}_x$ in the range $0.06 \leq x \leq 0.20$ have been shown by Möller and Drickamer⁴⁵ to exhibit strikingly different behavior from those of the present $\text{Pd}_{1-x}\text{Co}_x$ alloys. The PdFe Curie temperatures have very little pressure dependence, dT_C/dp being perhaps slightly negative toward the higher concentrations (of order $\sim -0.05 \text{ }^\circ\text{K/kbar}$), in contrast to the strongly positive pressure dependence for PdCo shown in Table I. The PdFe hyperfine fields at room temperature exhibit none of the dramatic effects observed for PdCo : the fields $|H_i|$ for $x = 0.20$ and 0.16 decrease slightly at low pressures,

then increase again above ~ 80 kbar, while $|H_i|$ for $x = 0.13$ decreases monotonically with pressure, most rapidly at the lower pressures. (See Fig. 1 of Ref. 45.) Since T_C for the PdFe alloys having $x \lesssim 0.12$ is below room temperature, no hyperfine field was observed for those cases, similarly to the situation for PdCo with $x \lesssim 0.08$ in this work.

We first consider the hyperfine fields. Assuming the maximum pressure dependence of the Curie temperatures allowed by the experimental uncertainties in Ref. 45, the pressure-dependent hyperfine fields for $\text{Pd}_{1-x}\text{Fe}_x$ in Ref. 45 can be plotted in the manner of Fig. 4. This is done in Fig. 8, for the alloys $x = 0.13, 0.16,$ and 0.20 . For reference in Fig. 8 the following spontaneous-magnetization curves are also plotted: $\sigma(T)/\sigma_0$ for ferromagnetic iron and $f(T/T_C)$ from the molecular-field theory with $S = \frac{1}{2}$ and $\frac{3}{2}$. The saturation values $H_0(p=0)$ for the PdFe alloys are taken from Craig *et al.*,¹⁸ who have fitted the composition dependence of $H_0(p=0)$ for Fe^{57} in this alloy system over the entire composition range.

The experimental curves of Fig. 8 indeed have little in common with those of Fig. 4. The major disparity results from the differences of $T_C(p)$ in the two systems. In fact the small pressure dependence of T_C has little effect on the hyperfine fields of the $x = 0.20$ and $x = 0.16$ PdFe alloys, whose behavior must be determined by the other two relevant parameters here: $\zeta(p)$ and $H_0(p)$. The effect of a decreasing $T_C(p)$ is felt by the $x = 0.13$ alloy, however, as seen in Fig. 8, and is the reason for the overall decrease of $|H_i|$ with pressure in that case. This result can be seen from Eqs. (4) and (A3), which indicate the effect of $T_C(p)$, with H_0 and ζ constant, is that $H_i(p)$ must follow its T -dependent $p = 0$ baseline $g_0(T/T_C)$. The large negative slope of the baseline for $x = 0.13$ (being in the region $T/T_C \lesssim 1$) thus imposes an overall negative slope on $|H_i(p)|$. The curvature of $|H_i(p)|$ relative to the baseline of the $x = 0.13$ curve is qualitatively the same as that of the higher-concentration alloys and must similarly result from the effects of $\zeta(p)$ and/or $H_0(p)$.

We expect the parameter $\zeta(p)$ to be relatively unimportant here, unlike the situation for the PdCo alloys where the Fe^{57} parent atom is a bona fide impurity, having, for instance, a different moment ($\sim 3\mu_B$) than the average Co atom ($\sim 2\mu_B$).^{5,6} This conclusion follows from the work of Craig *et al.*,²⁰ who have measured both $\sigma(T)/\sigma_0$ and $H_i(T)/H_0$ at $p = 0$ for Fe^{57} in the ferromagnetic alloy $\text{Pd}_{0.9735}\text{Fe}_{0.0265}$. They found an accurate proportionality to hold over extended ranges of temperature and applied external field, i. e., the thermal response of the impurity magnetization follows that of the host closely, as it does in pure ferromagnet-

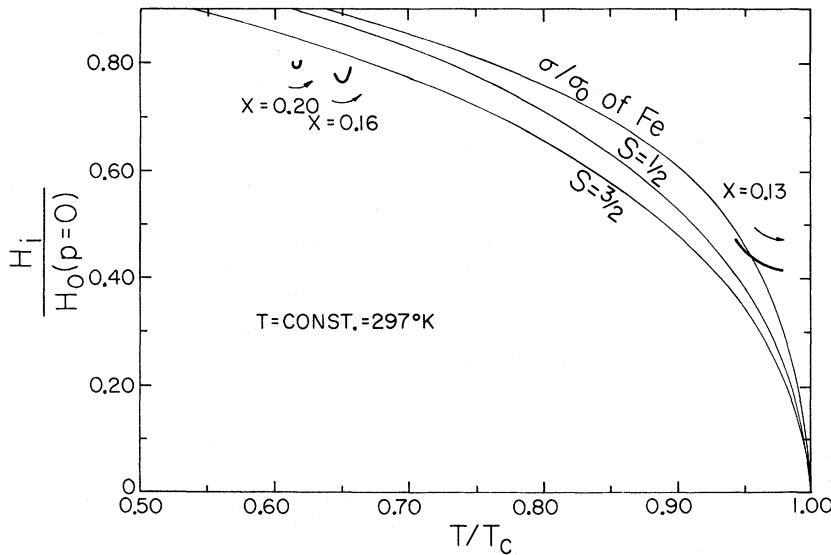


FIG. 8. Analog of Fig. 4 for Pd_{1-x}Fe_x alloys, from the data of Ref. 45 as described in the text. Also shown are the spontaneous-magnetization curve for iron and the molecular-field curves for spin- $\frac{1}{2}$ and spin- $\frac{3}{2}$.

ic iron, even for this relatively dilute PdFe alloy. The exchange field driving the Fe⁵⁷ "impurity" is thus determined mainly by the Fe moments which also drive the host, so even under pressure the *relative* response of impurity to host should not be significantly altered. This result should be particularly true at the higher concentrations 0.13 $\leq x \leq$ 0.20 considered in Fig. 8.

The shape of the curves $H_i(p)$, then, must result primarily from the effects of $H_0(p)$ which, as discussed earlier, is $A(p)\mu_0(p)$ for the localized impurity case or $A(p)\sigma_0(p)$ for the homogeneous case. The situation for Fe⁵⁷ in PdFe apparently lies somewhere between the above two extremes, since the Fe⁵⁷ hyperfine field is sensitive to the itinerant Pd 4d-band polarization as well as to the local 3d Fe moment.¹⁸ If, as expected, $d \ln A / dp > 0$ (as it is⁵⁸ for Fe⁵⁷ in Fe) and $d \ln \sigma_0 / dp < 0$ (as is known to be the case, for example, in Fe, Co, Ni, and PdNi^{58,41}), the nonlinearity in $H_0(p)$ indicates that either $A(p)$ or the appropriate combination of $\mu_0(p)$ and $\sigma_0(p)$ is nonlinear in p , with the decreasing moments dominating at low p and the increasing hyperfine-coupling constant dominating at higher p .

It is interesting to note that the situation observed here for $H_0(p)$ in PdFe and PdCo may be related to the fact that $d \ln H_0 / dp$ for Fe⁵⁷ in pure iron is negative,^{49,89} whereas in pure cobalt it is positive,⁸⁶ at least to moderate pressures.⁷⁸ According to the present ideas, for Fe⁵⁷ in cobalt, $H_0 = A\mu_0$, and the positive pressure dependence of $|A|$ dominates since the pressure dependence of $|\mu_0|$ is small; for Fe⁵⁷ in iron, $H_0 = A\sigma_0$, and the negative pressure dependence of $|\sigma_0|$ is dominant.

E. $T_C(p)$ for PdFe and PdCo

The qualitatively different pressure dependences observed for $T_C(p)$ in the PdFe and PdCo systems

over the composition range $0.05 \lesssim x \lesssim 0.20$ suggest a reexamination of the point of view taken previously in Ref. 44. In that work the composition dependence of dT_C/dp for the PdCo system was successfully fitted in terms of the dilute-impurity model of Takahashi and Shimizu¹³ and of Kim,¹⁴ with two adjustable parameters. If in fact the dilute-alloy model is applicable here, the implication is that the alloys PdCo and PdFe should behave similarly, since it is well known that the dilute PdCo and PdFe systems have very similar magnetic properties.^{9,10-14,77} On the other hand, in the nondilute regime significant differences appear. For example, as x increases toward 0.25 the composition dependences of the Curie temperatures, which are qualitatively the same for small x , differ radically: $T_C(x)$ for Pd_{1-x}Co_x continues to rise smoothly with x , while $T_C(x)$ for Pd_{1-x}Fe_x peaks at $\sim x = 0.25$ and then *decreases* with increasing x .⁷⁸ This behavior is reminiscent of the somewhat-analogous systems NiCo and NiFe: In the former case $T_C(x)$ rises smoothly with increasing x (despite the existence of an ordered phase at $x = 0.25$), while in the latter case $T_C(x)$ reaches a maximum near $x = 0.35$, then decreases.⁷⁹ This phenomenon in NiFe is associated with the onset of Invar effects, which occur notoriously in that alloy system but which do *not* occur in NiCo. Invar effects have also been observed in the system PdFe,⁸⁰⁻⁸² but not in PdCo. Thus, one expects *dissimilar* behavior from the nondilute alloys PdFe and PdCo. The fact that the quantities dT_C/dp for the two systems are quite different in the concentration range under consideration suggests this to be a nondilute regime, where direct impurity-impurity interactions (i. e., Fe-Fe or Co-Co) are significant.⁸³

The sign of the qualitative difference of dT_C/dp in the two systems supports the above picture. The

invar effects in FeNi are thought to result from an antiferromagnetic direct Fe-Fe exchange interaction occurring in the fcc structure,^{84,85} and it has been observed that pressure tends to strengthen this antiferromagnetic interaction at the expense of ferromagnetic interactions.^{85,86} Thus T_C is suppressed by pressure in a ferromagnetic Invar-type alloy, or the Néel temperature T_N is enhanced if the alloy is antiferromagnetic. This effect has been observed in the fcc Fe-rich alloys $FePd$ ⁸⁷ and is consistent with the data of Möller and Drickamer in the fcc Pd-rich system $PdFe$; i. e., relative to the strongly positive pressure dependence of $T_C(p)$ in $PdCo$, the pressure dependence of $T_C(p)$ in $PdFe$ is small or weakly negative. Conceivably Invar-type Fe-Fe interactions in the nondilute $PdFe$ alloys tend to force T_C down with pressure, suppressing dT_C/dp below the positive values appearing in $PdCo$ where such interactions are not present.⁸⁸

In the dilute alloys the pressure derivatives dT_C/dp appear to be negative: Fawcett *et al.*³³ have found $dT_C/dp = -(4 \pm 4) \times 10^{-3}$ °K/kbar for $Pd_{0.997}Fe_{0.003}$ and $-(0.10 \pm 0.04)$ °K/kbar for $Pd_{0.97}Fe_{0.03}$, while Christoe *et al.*⁸⁹ have measured $dT_C/dp = -(0.09 \pm 0.01)$ °K/kbar for $Pd_{0.97}Fe_{0.03}$ (averaged from 0 to 60 kbar). Fawcett *et al.*³³ have also found $dT_C/dp = (0.0 \pm 0.1)$ °K/kbar for $Pd_{0.97}Co_{0.03}$. If, as expected, the dilute alloys behave similarly with pressure, then dT_C/dp is negative in dilute $PdCo$. The positive dT_C/dp seen in the higher-concentration $PdCo$ alloys is then similar to the situation in $PdNi$, where $dT_C/dp < 0$ for the dilute alloys and then increases with x , becoming positive for $x \geq 0.20$.⁴⁰ According to the above arguments involving the differences between the systems $PdCo$ and $PdFe$ at moderate concentrations, the behavior observed for $T_C(p)$ of $PdCo$ in Ref. 44 must be characteristic of the nondilute regime, hence involving direct impurity-impurity interactions which are not treated by the model used in Ref. 44. Thus the fit afforded by the dilute-alloy model in Ref. 44, although sufficient, may not be necessary, and we note that a treatment involving directly interacting impurities^{15,71,90-93} might be more appropriate.

Before concluding we briefly present the pressure-dependent Fe^{57} isomer shifts for the current fcc $PdCo$ alloys, at 297 °K, in Fig. 9. The data of Ingalls *et al.*⁹⁴ for Fe^{57} in pure Pd (fcc) and Co (hcp) are also indicated. The $PdCo$ results are seen to be composition-independent and coincident with the Pd and Co data within experimental accuracy. The similarity of the pressure dependences of Fe^{57} isomer shifts in close-packed transition metals, noted by Ingalls *et al.*,⁹⁴ is maintained here. A more complete discussion of the effects of pressure on Fe^{57} isomer shifts in transition metals is given in Ref. 75.

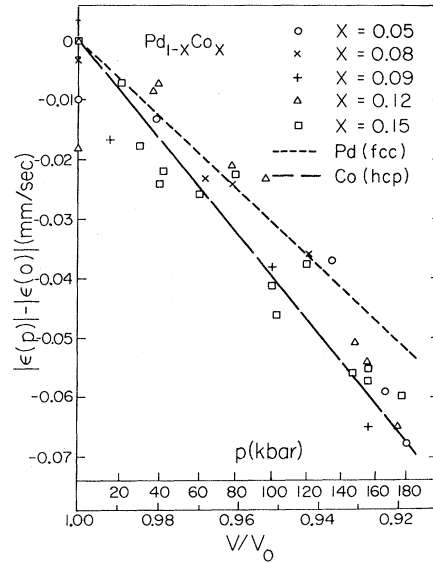


FIG. 9. Pressure and volume dependences of Fe^{57} isomer shifts ϵ in $PdCo$ alloys at 297 °K. Dashed and dotted lines are from Ref. 94.

V. CONCLUSION

In this work we have shown that the dramatic effects observed for the pressure-dependent Fe^{57} hyperfine fields at 297 °K in a series of $Pd_{1-x}Co_x$ alloys (with $x \approx 0.08, 0.09, 0.12,$ and 0.15) are due partially to the positively pressure-dependent Curie temperatures (cf. Fig. 4), but not entirely. Account must also be taken of the pressure dependences of the zero-temperature hyperfine field and of the host-impurity coupling constant. This coupling constant was first introduced by Jaccarino *et al.*⁹⁰ in a molecular-field treatment and is expected to be physically meaningful when the impurity has a localized well-formed moment (as seems to be the case for Fe^{57} in $PdCo$ ^{5,6,72,16}) which is not too strongly coupled to the host magnetization.⁶² We have shown that the present data can be fitted semiquantitatively in the molecular-field approximation with two composition-independent parameters: $d \ln H_0/dp \approx +(1.0 \pm 0.5) \times 10^{-3}/kbar$ and $d \ln g/dp \approx -(3 \pm 1) \times 10^{-3}/kbar$, and have noted that this fit is unique if the composition independence is assumed to be necessary, as seems reasonable. To our knowledge, a pressure-dependent host-impurity coupling constant has not been seen before in any metal. It was observable here only through the consistency requirements set by the series of alloys investigated.

Although it is not impossible that the effects seen here are related to Fe-clustering phenomena as described by Ferrando *et al.*²⁹ and Rubenstein³⁰ for Fe^{57} in ferromagnetic $PdNi$ alloys, this pos-

sibility can be regarded as unlikely for several reasons: (i) The Fe⁵⁷-clustering effects in PdNi were observed to disappear after long annealing times of several days. The annealing period here was still longer and at comparable temperatures. (ii) Since the alloy systems PdCo, PdFe, and CoFe are all random substitutional alloys, it is unlikely that the present ternary system PdCo(Fe) would tend to segregate under long annealing periods. (iii) The two distinct sets of hyperfine field patterns observed by Ferrando *et al.* as indicative of clustered and nonclustered Fe⁵⁷ were not seen here. Another possibility that the pressure effects observed in this work are related to demagnetizing effects of the foil samples and thus are not true microscopic phenomena can also be discounted. Although the foil samples are plastically deformed in the course of a pressure run (mainly they are squeezed thinner), the effects observed here are completely reversible, as noted earlier, and thus cannot be a function of the sample shape.

In parametrizing the finite-temperature impurity hyperfine-field problem for the present case of Fe⁵⁷ in PdCo, we have shown that the positive pressure dependence of $|H_0|$ is probably due mainly to the positive pressure dependence of the hyperfine coupling constant $|A|$. The negative pressure dependence of $|\zeta|$ indicates that the Fe⁵⁷ impurity moment becomes progressively uncoupled from the host magnetization as the pressure increases. Comparison of the PdCo data with PdFe indicates that the positive pressure dependence of the Curie temperatures in this concentration regime is due, at least partially, to direct impurity-impurity interactions.

An important result of this work is the demonstration of the importance of impurity effects in measurements of the pressure dependence of impurity hyperfine fields in metals, particularly at finite temperatures. A similar importance of impurity effects has recently been discussed in relation to the pressure dependence of Fe⁵⁷ isomer shifts in transition and noble metals.⁷⁵ Thus although one might expect to gain information on the pressure-dependent properties of the PdCo alloys via the magnitudes of the Fe⁵⁷ hyperfine fields, it is apparent here that one observes mainly the pressure-dependent properties of the Fe⁵⁷ impurity state itself and of its interaction with the host, through the pressure dependences of the coupling constants A and ζ .⁹⁵

ACKNOWLEDGMENTS

The authors wish to acknowledge the cooperation and skill of G. DePasquali in the preparation of the Mössbauer sources. We also thank J. G. Booth of the Battelle Memorial Institute for synthesizing samples, P. A. Beck for help with the metallurgy,

and M. Cohen and K. R. Reddy for stimulating discussions. One of us (J. A. C.) performed essentially all of the analysis while at the Department of Physics, University of Pennsylvania.

APPENDIX

It seems not to be generally appreciated that the Brillouin-related molecular-field spontaneous-magnetization functions can be easily calculated to any desired degree of accuracy without recourse to graphical solutions or computers, if only the Brillouin functions themselves are available with sufficient accuracy. The procedure is simply to calculate the quantity

$$\tau(x) = \frac{3S}{S+1} \frac{B_S(x)}{x} \quad (\text{A1})$$

from the given $B_S(x)$. $\tau(x)$ here is just T/T_C , and a plot of $B_S(x)$ vs $\tau(x)$ is exactly the spontaneous-magnetization function $\sigma(T)/\sigma_0$ vs T/T_C for spin S , i. e., the function $f(T/T_C)$. The price paid for this ease of calculation is that the independent variable is x (implicitly) instead of T/T_C , which is a minor inconvenience.

The impurity response function $g(T/T_C)$ of Eq. (5) can also be calculated simply, by an extension of the above implicit method, if the host spontaneous-magnetization function $f(T/T_C)$ is expressed within the molecular-field theory. $g(T/T_C)$ is then given exactly by a plot of

$$B_{S'}\left(\frac{S+1}{3S}\zeta x\right) \text{ vs } \tau(x), \quad (\text{A2})$$

where $\tau(x)$ is the same as in Eq. (A1). Here S is the effective spin/atom of the host, S' is the impurity spin, and ζ is the impurity-host coupling parameter of Eq. (5). Note that when $S' = S$ and $\zeta = 3S/(S+1)$ the impurity's response is just that of the host itself, so that $g(T/T_C) = f(T/T_C)$.

In some situations it is desirable to generate a family of the ζ -dependent functions $g(T/T_C)$ from a given experimental $g(T/T_C)$, the host function $f(T/T_C)$ being unknown. For example, as mentioned in the text, a temperature-dependent measurement of the Fe⁵⁷ hyperfine field in a given alloy at $p = 0$ would give a zero-pressure function, say, $g_0(T/T_C)$, from Eq. (4). In order to investigate the behavior of the parameter $\zeta(p)$ it is then necessary to obtain the family of curves $g(T/T_C)$ related to $g_0(T/T_C)$ by simple variation of the parameter ζ , as in Fig. 7. From Eq. (5), this can be done according to

$$g(T/T_C) = B_{S'}\left(\frac{\zeta}{\zeta_0} B_{S'}^{-1}(g_0(T/T_C))\right), \quad (\text{A3})$$

where ζ_0 is the (unknown) value of ζ in $g_0(T/T_C)$, S' is the impurity spin, and $B_{S'}^{-1}$ is an inverse Brill-

loun function. The parameter ζ associated with the generated function $g(T/T_C)$ is not known completely here—only the ratio ζ/ζ_0 is known—but

since one is generally interested in logarithmic pressure (or volume) derivatives, this ratio is all that is required.

*Work supported in part by the U. S. Atomic Energy Commission under Contract No. AT (11-1)-1198.

[†]Present address: Department of Physiology and Biophysics, University of the Pacific, San Francisco, Calif. 94115 and Cardiovascular Research Institute, School of Medicine, University of California, San Francisco, Calif. 94122.

- ¹F. W. Constant, *Phys. Rev.* **36**, 1654 (1930).
²D. Gerstenberg, *Ann. Phys. (Leipz.)* **2**, 236 (1958).
³R. M. Bozorth, P. A. Wolff, D. D. Davis, V. B. Compton, and J. H. Wernick, *Phys. Rev.* **122**, 1157 (1961).
⁴J. Crangle, *Philos. Mag.* **5**, 335 (1960).
⁵J. W. Cable, E. O. Wollan, and W. C. Koehler, *Phys. Rev.* **138**, A755 (1965).
⁶G. G. Low and T. M. Holden, *Proc. Phys. Soc. Lond.* **89**, 119 (1966).
⁷T. J. Hicks, T. M. Holden, and G. G. Low, *J. Phys. C* **1**, 528 (1968).
⁸G. G. Low, *Adv. Phys.* **18**, 371 (1969).
⁹B. Giovannini, M. Peter, and J. R. Schrieffer, *Phys. Rev. Lett.* **12**, 736 (1964).
¹⁰A. M. Clogston, *Phys. Rev. Lett.* **19**, 583 (1967).
¹¹D. J. Kim and B. B. Schwartz, *J. Appl. Phys.* **40**, 1208 (1969).
¹²T. Moriya, *Prog. Theor. Phys.* **34**, 329 (1965).
¹³T. Takahashi and M. Shimizu, *J. Phys. Soc. Jap.* **20**, 26 (1965).
¹⁴D. J. Kim, *Phys. Rev.* **149**, 434 (1966).
¹⁵D. J. Kim, *Phys. Rev. B* **1**, 3725 (1970).
¹⁶D. E. Nagle, P. P. Craig, P. Barrett, D. R. F. Cochran, C. E. Olsen, and R. D. Taylor, *Phys. Rev.* **125**, 490 (1962).
¹⁷P. P. Craig, D. E. Nagle, W. A. Steyert, and R. D. Taylor, *Phys. Rev. Lett.* **9**, 12 (1962).
¹⁸P. P. Craig, B. Mozer, and R. Segnan, *Phys. Rev. Lett.* **14**, 895 (1965).
¹⁹T. A. Kitchens, W. A. Steyert, and R. D. Taylor, *Phys. Rev.* **138**, A467 (1965).
²⁰P. P. Craig, R. C. Perisho, R. Segnan, and W. A. Steyert, *Phys. Rev.* **138**, A1460 (1965).
²¹F. W. D. Woodhams, R. E. Meads, and J. S. Carlow, *Phys. Lett.* **23**, 419 (1966).
²²T. A. Kitchens and P. P. Craig, *J. Appl. Phys.* **37**, 1187 (1966).
²³W. L. Trousedale, G. Longworth, and T. A. Kitchens, *J. Appl. Phys.* **38**, 922 (1967).
²⁴M. P. Maley, R. D. Taylor, and J. L. Thompson, *J. Appl. Phys.* **38**, 1249 (1967).
²⁵B. D. Dunlap and J. G. Dash, *Phys. Rev.* **155**, 460 (1967).
²⁶N. A. Blum and R. B. Frankel, *J. Appl. Phys.* **39**, 959 (1968).
²⁷G. Longworth, *Phys. Rev.* **172**, 572 (1968).
²⁸T. A. Kitchens and W. L. Trousedale, *Phys. Rev.* **174**, 606 (1968).
²⁹W. A. Ferrando, R. Segnan, and A. I. Schindler, *J. Appl. Phys.* **41**, 1236 (1970); *Phys. Rev. B* **5**, 4657 (1972).
³⁰M. Rubenstein, *Solid State Commun.* **8**, 919 (1970).
³¹U. Erich, J. Göring, S. Hüfner, and E. Kankeleit, *Phys. Lett.* **A31**, 492 (1970).
³²F. E. Obenshain, W. A. Glaeser, G. Czyzek, and J. E. Tansil, *J. Phys. (Paris) Suppl.* **32**, 783 (1971).
³³E. Fawcett, D. B. McWhan, R. C. Sherwood, and M. P. Sarachik, *Solid State Commun.* **6**, 509 (1968).
³⁴E. Fawcett, E. Bucher, W. F. Brinkman, and J. P. Maita, *Phys. Rev. Lett.* **21**, 1183 (1968).
³⁵E. Fawcett and R. C. Sherwood, *Phys. Rev. B* **1**, 4361 (1970).
³⁶E. Fawcett, *Phys. Rev. B* **3**, 3023 (1971).

³⁷M. Matsumoto, T. Goto, and T. Kaneko, *J. Phys. (Paris) Suppl.* **32**, 419 (1971).

³⁸E. Tatsumoto, T. Okamoto, S. Ishida, and J. Ishida, *J. Phys. Soc. Jap.* **24**, 950 (1968).

³⁹J. Ishida and S. Ishida, *J. Sci. Hiroshima Univ.* **33**, 257 (1969).

⁴⁰E. Tatsumoto, H. Fujiwara, T. Okamoto, and H. Fujii, *J. Phys. Soc. Jap.* **25**, 1734 (1968).

⁴¹H. Fujiwara, N. Tsukiji, N. Yamate, and E. Tatsumoto, *J. Phys. Soc. Jap.* **23**, 1176 (1967).

⁴²H. Fujiwara, *J. Sci. Hiroshima Univ.* **31**, 177 (1967).

⁴³J. A. Cohen, thesis (University of Illinois, 1968) (unpublished).

⁴⁴W. B. Holzapfel, J. A. Cohen, and H. G. Drickamer, *Phys. Rev.* **187**, 657 (1969).

⁴⁵H. S. Möller and H. G. Drickamer, *J. Phys. Chem. Solids* **32**, 745 (1971).

⁴⁶*Constitution of Binary Alloys*, 2nd ed., edited by M. Hansen (McGraw-Hill, New York, 1958), p. 491.

⁴⁷W. H. Southwell, D. L. Decker, and H. B. Vanfleet, *Phys. Rev.* **171**, 354 (1968).

⁴⁸P. Debrunner, R. W. Vaughan, A. R. Champion, J. A. Cohen, J. A. Moyzis, and H. G. Drickamer, *Rev. Sci. Instrum.* **37**, 1310 (1966).

⁴⁹D. N. Pipkorn, C. K. Edge, P. Debrunner, G. DePasquali, H. G. Drickamer, and H. Frauenfelder, *Phys. Rev.* **135**, A1604 (1964).

⁵⁰E. A. Perez-Albuern, K. F. Forsgren, and H. G. Drickamer, *Rev. Sci. Instrum.* **35**, 29 (1964).

⁵¹B. L. Chrisman and T. A. Tumolillo, *Comput. Phys. Commun.* **2**, 322 (1971).

⁵²R. S. Preston, S. S. Hanna, and J. Heberle, *Phys. Rev.* **128**, 2207 (1962).

⁵³C. E. Violet and D. N. Pipkorn, *J. Appl. Phys.* **42**, 4339 (1971).

⁵⁴M. H. Rice, R. G. McQueen, and J. M. Walsh, in *Solid State Physics*, edited by F. Seitz and D. Turnbull (Academic, New York, 1958), Vol. 6, p. 1.

⁵⁵The compressibility is expected to have an anomaly around $T = T_C$, since it is a second derivative of the thermodynamic potential and should thus be discontinuous at a second-order phase-transition critical point [K. P. Belov, *Magnetic Transitions* (Consultants Bureau, New York, 1961), pp. 1 and 2]. From the data of Ref. 38 on the alloy Pd_{0.795}Ni_{0.205} it appears that the difference in volume compressibilities of the paramagnetic and ferromagnetic phases is of order $\Delta\kappa \sim 0.3 \times 10^{-4}$ /kbar, the paramagnetic phase being the more compressible. If applied to the present alloys, this figure implies a difference in V/V_0 of $\sim 0.6\%$ at 200 kbar between an alloy which is ferromagnetic and one which is not. Since the over-all volume changes here are of order 10% at 200 kbar, the above effect is negligible.

⁵⁶D. H. Martin, *Magnetism in Solids* (MIT, Cambridge, Mass., 1967).

⁵⁷J. S. Smart, *Effective Field Theories of Magnetism* (Saunders, Philadelphia, Pa., 1966).

⁵⁸D. H. Anderson, *Solid State Commun.* **4**, 189 (1966).

⁵⁹K. J. Duff and T. P. Das, *Phys. Rev. B* **3**, 2294 (1971).

⁶⁰V. Jaccarino, L. R. Walker, and G. K. Wertheim, *Phys. Rev. Lett.* **13**, 752 (1964).

⁶¹H. Callen, D. Hone, and A. J. Heeger, *Phys. Lett.* **17**, 233 (1965).

⁶²D. Hone, H. Callen, and L. R. Walker, *Phys. Rev.* **144**, 283 (1966).

⁶³J. G. Dash, B. D. Dunlap, and D. G. Howard, *Phys. Rev.* **141**, 376 (1966).

⁶⁴I. A. Campbell, *J. Phys. C* **3**, 2151 (1970).

- ⁶⁵This point has been demonstrated experimentally for Fe^{57} in PdFe in Ref. 23.
- ⁶⁶D. L. Raimondi and G. Jura, *J. Appl. Phys.* **38**, 2133 (1967).
- ⁶⁷D. H. Martin, in Ref. 56, p.10.
- ⁶⁸J. M. Leger, C. Susse, and B. Vodar, *Solid State Commun.* **5**, 755 (1967).
- ⁶⁹J. D. Litster and G. B. Benedek, *J. Appl. Phys.* **34**, 688 (1963).
- ⁷⁰R. E. Watson and A. J. Freeman, *Phys. Rev.* **123**, 2027 (1961); Fig. 2.
- ⁷¹T. Moriya, in *Theory of Magnetism in Transition Metals*, edited by W. Marshall (Academic, New York, 1967), p. 206.
- ⁷²M. F. Collins and J. B. Forsyth, *Philos. Mag.* **8**, 401 (1963).
- ⁷³L. R. Walker, G. K. Wertheim, and V. Jaccarino, *Phys. Rev. Lett.* **6**, 98 (1961).
- ⁷⁴*Mössbauer Effect Data Index, 1958-1965*, edited by A. H. Muir, Jr., K. J. Ando, and H. M. Coogan (Interscience, New York, 1966), p. 26.
- ⁷⁵J. A. Cohen (unpublished).
- ⁷⁶H. G. Drickamer, R. L. Ingalls, and C. J. Coston, in *Physics of Solids at High Pressures*, edited by C. T. Tomizuka and R. M. Emrick (Academic, New York, 1965), p. 313.
- ⁷⁷A. D. C. Grassie, G. A. Swallow, G. Williams, and J. W. Loram, *Phys. Rev. B* **3**, 4154 (1971).
- ⁷⁸Reference 46, pp. 491 and 697.
- ⁷⁹Reference 46, pp. 486 and 678.
- ⁸⁰A. Kussmann and K. Jessen, *J. Phys. Soc. Jap. Suppl.* **17**, 136 (1963).
- ⁸¹H. Fujimori and H. Saito, *J. Phys. Soc. Jap.* **20**, 293 (1965).
- ⁸²S. K. Sidorov and A. V. Doroshenko, *Phys. Status Solidi* **16**, 737 (1966).
- ⁸³The anomalous behavior of $T_c(x)$ for PdFe could be associated with the existence of an ordered phase Pd_3Fe at $x = 0.25$. It is not clear at present whether a similarly ordered phase Pd_3Co exists in PdCo [Y. Matsuo and F. Hayashi, *J. Phys. Soc. Jap.* **28**, 1375 (1970)]. Whatever the reason for the unusual curvature of $T_c(x)$ in PdFe , the conclusion remains that the *nondilute* PdFe and PdCo alloys indeed have different magnetic properties.
- ⁸⁴E. I. Kondorsky and V. L. Sedov, *J. Appl. Phys. Suppl.* **31**, 331 (1960).
- ⁸⁵D. R. Rhiger and R. Ingalls, *Phys. Rev. Lett.* **28**, 749 (1972).
- ⁸⁶J. B. Goodenough, *Magnetism and the Chemical Bond* (Interscience, New York, 1963), p. 329.
- ⁸⁷R. C. Wayne and L. C. Bartel, *Phys. Lett.* **A28**, 196 (1968).
- ⁸⁸If the suppression of $T_c(x)$ in PdFe relative to PdCo is due primarily to the chemical ordering of Pd_3Fe near $x = 0.25$ and not to invar effects, then the present results imply that pressure stabilizes the ordered phase Pd_3Fe relative to the disordered phase $\text{Pd}_{0.75}\text{Fe}_{0.25}$.
- ⁸⁹C. W. Christoe, A. Forster, and W. B. Holzapfel, *Z. Phys.* **31**, 263 (1971).
- ⁹⁰S. Alexander and P. W. Anderson, *Phys. Rev.* **133**, A1594 (1964).
- ⁹¹T. Moriya, *Prog. Theor. Phys.* **33**, 157 (1965).
- ⁹²M. Inoue and T. Moriya, *Prog. Theor. Phys.* **38**, 41 (1967).
- ⁹³S. H. Liu, *Phys. Rev.* **163**, 472 (1967).
- ⁹⁴R. Ingalls, H. G. Drickamer, and G. DePasquali, *Phys. Rev.* **155**, 165 (1967).
- ⁹⁵It should be noted that measurements of $T_c(p)$ by Fe^{57} Mössbauer thermal scanning *do* yield direct information on the properties of the host which, neglecting relaxation phenomena, are not complicated by impurity effects [cf. Eqs. (2) and (4)].

Theory of Nuclear Quadrupole Interaction in Nontransition Metals—Magnesium*

P. Jena

Department of Physics, Dalhousie University, Halifax, Nova Scotia, Canada

and

S. D. Mahanti

Department of Physics, Michigan State University, East Lansing, Michigan 48823

and

T. P. Das

Department of Physics, State University of New York, Albany, New York 12203

(Received 21 August 1972)

A theoretical investigation of various electronic contributions to the electric field gradient in hcp magnesium has been carried out. The dominant contribution comes from the anisotropic filling of the \bar{k} space and is therefore a Fermi-volume effect. In contrast, the contribution associated with the distortion of the Fermi surface by the $l=2$ component of the lattice potential is found to be extremely small. The total electronic contribution is $0.0046e\alpha_0^3$ and anti-shields the lattice contribution of $0.0018e\alpha_0^3$.

I. INTRODUCTION

The nature of crystalline fields in noncubic metals is of considerable experimental and theoretical interest. For example, the nuclear quadrupole interaction¹ depends upon the electric field gradient (EFG) at the nucleus and its study provides information about the $l=2$ component of the crystalline

field. Furthermore, spin-resonance studies² of rare-earth impurities in noncubic metals provide valuable information about the nature of the crystalline fields in these metals.

In the present paper we investigate the nature of the $l=2$ component of the crystalline field by analyzing the electronic and lattice contributions to the EFG in magnesium. In contrast to other hyperfine